

## ARTICLE

# Energy Economic Dispatch for Photovoltaic–Storage via Distributed Event-Triggered Surplus Algorithm

Kaicheng Liu<sup>1,3</sup>, Chen Liang<sup>2</sup>, Naiyue Wu<sup>1,3</sup>, Xiaoyang Dong<sup>2</sup> and Hui Yu<sup>1,\*</sup>

<sup>1</sup>China Electric Power Research Institute, Beijing, 100192, China

<sup>2</sup>Electric Power Research Institute of State Grid Gansu Electric Power Company, Lanzhou, 730000, China

<sup>3</sup>State Key Laboratory of Power Grid Safety, Beijing, 100084, China

\*Corresponding Author: Hui Yu. Email: yuhui4813ncu@163.com

Received: 24 January 2024 Accepted: 19 April 2024 Published: 19 August 2024

## ABSTRACT

This paper presents a novel approach to economic dispatch in smart grids equipped with diverse energy devices. This method integrates features including photovoltaic (PV) systems, energy storage coupling, varied energy roles, and energy supply and demand dynamics. The system model is developed by considering energy devices as versatile units capable of fulfilling various functionalities and playing multiple roles simultaneously. To strike a balance between optimality and feasibility, renewable energy resources are modeled with considerations for forecasting errors, Gaussian distribution, and penalty factors. Furthermore, this study introduces a distributed event-triggered surplus algorithm designed to address the economic dispatch problem by minimizing production costs. Rooted in surplus theory and finite time projection, the algorithm effectively rectifies network imbalances caused by directed graphs and addresses local inequality constraints. The algorithm greatly reduces the communication burden through event triggering mechanism. Finally, both theoretical proofs and numerical simulations verify the convergence and event-triggered nature of the algorithm.

## KEYWORDS

Fully distributed algorithm; economic dispatch; directed graph; renewable energy resource

## 1 Introduction

The smart grid, conceptualized as the forthcoming paradigm for electrical power systems, aspires to realize operations that are optimally efficient, inherently flexible, profoundly secure, and consistently reliable. In this context, economic dispatch, which directly affects system operating costs, has become a problem that the smart grid needs to face, attracting considerable attention from the research community in recent years [1]. The economic dispatch problem (EDP) focuses on the allocation of energy generation devices or loads in a manner that minimizes system costs, while ensuring a balance between supply and demand and adhering to local boundary constraints. In essence, the EDP is an optimization problem which aims at maximizing the total social welfare while satisfying the constraint condition of global and local. It involves making system-level decisions and necessitates the development of efficient optimization algorithms.

To foster the sustainable advancement of energy and the environment, it is proposed that the EDP transition from the smart grid paradigm to an energy internet framework [2]. Concurrently, the



integration of substantial renewable energy sources introduces complexities into the energy system, manifesting as uncertainties in aggregate production and multi-timescale consumption. The energy storage capacity also increases along with the total amount of renewable energy. Literature [3] proposes the goal of “zero” carbon electricity consumption based on building parks, and energy storage capacity is saved by energy complementarity between building complexes. Meanwhile, literature [4] integrates hydrogen storage equipment into the existing power system to realize the coordinated operation of coupled units such as gas turbines and gas to power (G2P) facilities. In order to solve the multi-energy coupling problem of energy internet, literature [5,6] solves the balanced scheduling of cogeneration and electric-thermal integrated system using a new multicarrier energy system cogeneration optimization planning and game theory, respectively. From the above, it can be seen that the economic scheduling problem has received extensive attention regardless of the smart grid or energy internet.

Due to the decentralization of distributed algorithms, they play a great role in the economic scheduling process of the smart grid. Distributed methods can leverage neighbor node information to achieve distributed coordination among components within a network, effectively addressing challenges posed by large-scale systems, massive data, and time-varying characteristics [7]. Drawing from the principles of gradient descent and multi-agent consensus, scholars have introduced various distributed optimization algorithms to address the economic dispatch challenge in smart grids. For example, reference [8] recasts the economic dispatch issue in power systems as a convex quadratic function optimization dilemma, employing a gradient descent algorithm for its resolution. However, the method requires a leader to predict the degree of global supply-demand mismatch. So such algorithms are considered as incomplete distributed optimization algorithms. Literature [9] proposes a fully distributed optimization method, which does not rely on a leader or a cloud controller, and the optimal solution can be obtained for any strongly connected communication topology network. In [10], in order to address the influence of line losses in the energy transmission process, two consistency algorithms are combined to predict the degree of global power mismatch while obtaining the optimal Lagrange multipliers, respectively. Literature [11] considers the impact of customer demand side and explored the problem of economic dispatch of power system from a new perspective. To reduced convergence time and robustness of applications such as smart grid and energy internet, researchers have proposed the distributed consensus alternating direction method of multipliers (ADMM) algorithm [12,13]. In addition to this, there is a consensus-based approach that focuses on building distributed Lagrangian dyadic variables and ensuring that they converge to meet the optimality conditions. Various consensus-based algorithms have emerged in Table 1, including distributed Newton descent [14,15], distributed neurodynamics methods [16,17] and surplus-based optimization algorithms [18,19]. For literature [8,10,12,13,15–17], this paper uses surplus based distributed optimization algorithms and event triggering for directed graphs and communication cost reduction. Similarly, literature [18,19] still uses continuous communication without reducing the communication cost. Although literature [15] also uses event triggering to reduce the communication frequency and cost, it cannot do anything about the imbalance constraint problem caused by the undirected graph. And the proposed algorithm in this paper considers all the above problems.

**Table 1:** Comparative technical features of previous researches

Reference	Method	Communication structure	Reduced communication
[12,13]	ADMM	Undirected graph	None
[8,10,14]	Gradient descent	Undirected graph	None

(Continued)

**Table 1 (continued)**

Reference	Method	Communication structure	Reduced communication
[15]	Newton descent	Undirected graph	Event trigger
[16,17]	Neurodynamics	Undirected graph	None
[18,19]	Surplus-based	Directed graph	None
This paper	Surplus-based	Directed graph	Event trigger

With the advancement of distributed technologies and the extensive integration of renewable energy sources, the conventional power system is evolving into a smart grid. This transformation has brought new challenges for smart grid economic dispatch [20]. Firstly, communication capabilities have been added to each power generation device, which provides the basic conditions for distributed computing but also increases the risk of device privacy leakage. Second, renewable energy, as an uncontrollable energy source, has a high degree of uncertainty. In order to compensate for the loss caused by uncertainty, controllable energy sources need to cooperate with uncontrollable energy sources. This greatly increases the difficulty of economic dispatch. Moreover, devices in the smart grid can be both consumers and suppliers [21]. This leads to the diversification of the forms of energy producers and consumers. Additionally, smart grid must adhere to plug-and-play principles and account for variability in network topology. Hence, there is a need for the development of distributed methods to solve the EMP in the smart grid. Currently, the existing distributed computing methods are unable to meet the economic scheduling requirements of smart grids. In addition, for renewable energy sources such as photovoltaic (PV) power generation, PV-storage is usually used in conjunction to abate the uncertainty of PV power generation, fast system power fluctuations, and timeliness. In order to effectively reduce the cost of PV power generation and energy storage in the scheduling process, scholars have put forward higher requirements for PV power generation cost models, energy storage models and distributed algorithms. So, this paper addresses the above problems and challenges with the following main contributions:

1. We present a novel distributed event-triggered optimization algorithm specifically designed for photovoltaic power generation and energy storage devices. Compared to integrated energy systems involving electrical heat and cold multiple energy devices more specific, and due to the presence of multiple photovoltaic and energy storage devices, a single device lacks full-duplex information interaction, to the directed graph information topology of the distributed optimization challenges. Unlike existing methods, our approach utilizes dynamics and residual values to enable distributed optimization in directed graphs;
2. Photovoltaic power plants with volatility and unpredictability are non-dispatchable units; therefore, the inclusion of renewable energy models in the economic dispatch problem cannot be considered more specifically by simply treating their cost functions as quadratic. To model renewable energy resources, factors such as forecasting errors, Gaussian distribution, and penalty factors are taken into renewable energy cost function. By incorporating penalties for curtailing renewable generation, a balance can be achieved between optimality and generation feasibility, achieving dispatch ability of renewable energy devices;
3. The process of node information interaction incurs communication costs due to factors such as communication frequency. To minimize communication costs, we propose a distributed dispatch approach that integrates an event-triggered communication strategy. This strategy uses

parallel triggering to reduce the communication frequency without affecting the optimization performance of the algorithm. Meanwhile, this paper provides a complete theoretical proof process and digital simulation experiments.

The rest of this paper is arranged as follows. In [Section 2](#), we present an economic dispatch optimization model for PV-storage system. [Section 3](#) describes the distributed surplus optimization algorithm and the design process of the event-triggered strategy. Further, [Section 4](#) gives simulation experiments for the models and algorithms proposed in this paper to compare and analyze the performance and advantages. [Section 5](#) summarizes the main contents of this paper.

## 2 System Model and Problem Function

The smart grid infrastructure consists of a wide variety of distributed generation devices. Distributed generation devices can be categorized into three main groups: distributed renewable generator (DRG), distributed fuel generator (DFG), and distributed power storage device (DPSD). Photovoltaic power generator (PV), which are an integral part of DRG, are typically connected to DPSD and are jointly connected to the grid. However, due to the presence of multiple PV and DPSD, individual devices lack full-duplex information interaction. This presents a challenge when dealing with the distributed optimization of directed graph information topology graphs.

In order to enable distributed computation, bus nodes are treated as agents and connected to form a distributed communication network. The communication network of the entire system is defined as  $G = (V, \xi, A)$ , where  $V = \{1, 2, \dots, n\}$  represents the set of information nodes,  $\xi \subseteq V \times V$  is the set of communication lines within the system. The graph  $G$  is assumed to be strongly connected without self-loops. The adjacency matrix  $A = [a_{ij}]$  represents the connections between nodes, where  $a_{ij}$  is the element in the  $i$ th row and  $j$ th column of  $A$ . If node  $i$  can receive information from neighbor node  $j$ , there is an edge  $\xi_{ij}$  and  $a_{ij} = 1$ ; otherwise,  $a_{ij} = 0$ . The in-degree matrix  $D^{in} = \text{diag}[d_1^{in}, d_2^{in}, \dots, d_n^{in}]$  is defined as the diagonal matrix, where  $d_i^{in} = \sum_j^n a_{ij}$ . Similarly, the out-degree matrix  $D^{out} = \text{diag}[d_1^{out}, d_2^{out}, \dots, d_n^{out}]$  is defined as the diagonal matrix, where  $d_i^{out} = \sum_j^n a_{ji}$ . Additionally, we define the matrix  $L' = D^{out} - A$  and  $L = D - A$ . Because of the unbalanced and asymmetric nature of directed graphs, we can get  $L' \neq L$ .

### 2.1 PVs Model

When considering distributed renewable generators (DRGs), photovoltaics (PVs) play a crucial role as the main energy source, with no fuel cost involved. Photovoltaic power generation utilizes the principle of photoelectric properties of semiconductors, when there is light irradiation on the photovoltaic cell, it will produce electric. When light hits a photovoltaic cell, electron-hole pairs are generated, and the current increases as the number of pairs increases, thus realizing the direct conversion of light energy into electrical energy. However, it is essential to acknowledge that PVs cannot be treated as dispatchable units due to their intermittent and unpredictable nature. In order to add renewable energy sources to the EDP problem, we must only use forecasting techniques to obtain a rough of the likely generation of PVs. The mean forecasting value, derived from the day-ahead forecast curve provided by [18], is utilized as a reference for each scheduling horizon.

$$p_{i,t}^{PV,f} = \frac{1}{T} \int_t^{t+T} p_{i,\tau}^{PV,f} d\tau \quad (1)$$

where  $p_{i,t}^{PV,f}$  is the forecasting output of  $i$ th PV at time  $t$ ;  $T$  is the forecast period. Due to the existence of prediction errors, the true output value of PV may fluctuate up or down from the predicted

value. Therefore, we assume that the PV power generation error obeys a Gaussian distribution [19]. Moreover, according to the zero-waste renewable energy, we assume that all PV power is consumed. Furthermore, we set the confidence level to be  $100(1 - \delta)\%$ , where  $\delta$  is the corresponding significance. So we can get the confidence interval to  $[\bar{p}_{i,t}^{PV}, \underline{p}_{i,t}^{PV}]$ . Where  $\underline{p}_{i,t}^{PV} = p_{i,t}^{PV} - 3\sigma$  and  $\bar{p}_{i,t}^{PV} = p_{i,t}^{PV} + 3\sigma$ . Based on the previous discussion and the characterization of the Gaussian distribution, the cost function of PV is modeled as:

$$C(p_{i,t}^{PV}) = a_i p_{i,t}^{PV} - b_i \exp\left(c_i \frac{\bar{p}_{i,t}^{PV} - p_{i,t}^{PV}}{p_{i,t}^{PV} - \underline{p}_{i,t}^{PV}}\right) \quad (2)$$

where  $a_i$ ,  $b_i$  and  $c_i$  are the non-negative constants. The first item is the operation and maintenance cost of PV. The second item is the PV generation compensation due to the uncertainty of renewable energy. The more inaccurate the prediction results will lead to a larger compensation term.

**Remark 1:** Photovoltaic power plants with volatility and unpredictability are non-dispatchable units; therefore, the inclusion of renewable energy models in the economic dispatch problem cannot be considered more specifically by simply treating their cost functions as quadratic. Compared to fuel generators, the operating costs of PV are lower. However, due to the inaccuracy of PV forecasting, it is necessary for DFG to cooperate with PV generation to realize the balance between supply and demand of the system. This undoubtedly increases the generation cost of DFG, which needs to be borne by PV. Therefore, we establish the PV cost function, which is not only related to the operation and maintenance cost, but also related to the deviation between the real and predicted values. The larger the deviation, the larger the compromise that DFG needs to make, and thus the higher the compensation cost that PV needs to bear. And vice versa.

## 2.2 DFG Model

Distributed fuel generators (DFGs) use the heat from the combustion of flammable substances to heat and pressurize liquid water into water vapor. The steam is transported by a delivery tube to a turbine that drives a rotor to spin at a very high speed, which cuts off the magnetic field and generates electricity. To address and explore the ramping rate constraints of distributed fuel generators, the discrete version is typically transformed into a knapsack problem. The cost function of DFG is represented as follows:

$$C(p_i^{fg}) = a_i (p_i^{fg})^2 + b_i p_i^{fg} + c_i, \quad (3)$$

$$p_i^{fg,\min} \leq p_i^{fg} \leq p_i^{fg,\max}, \quad (4)$$

$$-p_i^{fg,ramp} \leq p_i^{fg}(t+1) - p_i^{fg}(t) \leq p_i^{fg,ramp}, \quad (5)$$

where  $p_i^{fg}$  is the power outputs of  $i$ th fuel-based generators;  $a_i$ ,  $b_i$  and  $c_i$  are the non-negative constants as cost coefficients;  $p_i^{fg,\min}$  and  $p_i^{fg,\max}$  are the minimum and maximum generator outputs, respectively;  $p_i^{fg,ramp}$  is the positive constant as ramp rate constraints, indicating that the DFG needs to be within a certain range to adjust the span of generation per unit of time.

## 2.3 DPSD Model

Let  $p_{i,t}^{ps}$  represent the store/release power,  $SOC_{i,t}^{ps}$  denote the stored energy of the  $i$ th distributed power storage device (DPSD) at time  $t$ . Here, we define  $p_{i,t}^{ps} > 0$  as discharging actions and  $p_{i,t}^{ps} < 0$  as charging actions. It is worth noting that the DPSD cannot be charged or discharged simultaneously. It must adhere to the following dynamic constraints:

$$-p_{i,t}^{ch,max} \leq p_{i,t}^{ps} \leq p_{i,t}^{ds,max} \quad (6)$$

$$SOC_{i,t}^{min} \leq SOC_{i,t}^{ps} \leq SOC_{i,t}^{max} \quad (7)$$

$$SOC_{i,t}^{ps} = SOC_{i,t-1}^{ps} - \left( \alpha_i^{ch} \beta_{i,t-1}^{ch} + \frac{1}{\alpha_i^{ds}} \beta_{i,t-1}^{ds} \right) p_{i,t-1}^{ps} T \quad (8)$$

$$\beta_{i,t-1}^{ch} + \beta_{i,t-1}^{ds} \leq 1 \quad (9)$$

Let  $p_{i,t}^{ch,max}$  and  $p_{i,t}^{ds,max}$  represent the maximum charging and discharging value. Additionally,  $SOC_{i,t}^{min}$  and  $SOC_{i,t}^{max}$  denote the lower and upper bounds for the allowed energy stored in the corresponding distributed power storage device (DPSD). The charging and discharging coefficients are represented by  $\alpha_i^{ch}$  and  $\alpha_i^{ds}$ , respectively. To distinguish the charging/discharging state of the DPSD, we denote  $\beta_{i,t-1}^{ch}, \beta_{i,t-1}^{ds} \in \{0, 1\}$ .  $\beta_{i,t-1}^{ch} = 1$  represents the charging state, while  $\beta_{i,t-1}^{ds} = 1$  represents the discharging state. To maximize social welfare, DPSDs are usually charged when electricity prices are low and discharged when prices are high. To capture these operations, the following cost function is utilized:

$$C(p_{i,t}^{ps}) = a_i (p_{i,t}^{ps} + b_i)^2 \quad (10)$$

where  $a_i$  and  $b_i$  are the cost coefficients.

### 3 Problem Formulation and Distributed Algorithm

This study primarily concentrates on the hourly economic dispatch problem (EMP) of the smart grid, aiming to achieve coordinated planning of distributed fossil generators (DFGs), photovoltaics (PVs), and distributed power storage devices (DPSD).

#### 3.1 Objective Function

To simplify the notation, we use  $\mathbb{R}^s$  to denote  $s$ -order real numbers and  $\mathbb{R}^+$  to denote the positive real numbers. The objective function represents the maximization of social welfare as well as the minimization of the cost of generating electricity at each facility, as depicted in Eqs. (11), (12). The objective function ensures compliance with the aforementioned inequality constraints and global equality constraints, as illustrated in Eqs. (13)–(15).

$$\min \quad Obj = f(p) \quad (11)$$

$$f(p) = \sum_1^n C_i(p_i^{pv}) + \sum_1^m C_i(p_i^g) + \sum_1^w C_i(p_i^{ps}) \quad (12)$$

$$s.t. \quad \sum_{i=1}^{n+m+w} p_i = \sum_{i=1}^{n+m+w} l_i \quad (13)$$

$$p_i^{min} \leq p_i(t) \leq p_i^{max} \quad (14)$$

$$|p_i(t+1) - p_i(t)| \leq p_i^{ramp} \quad (15)$$

where  $n, m, w$  are the number of PVs, DFGs and DPSDs.  $p_i \in [p_1^{pv}, \dots, p_n^{pv}, p_1^g, \dots, p_m^g, p_1^{ps}, \dots, p_w^{ps}]$  is the amount of power generated by the device,  $p_i^{max}$  and  $p_i^{min}$  denote the maximum and minimum power generation of the device, corresponding to the boundary constraints of the device mentioned earlier.  $l_i$  denotes the load of each node. Further, Eqs. (14) and (15) can be transformed into the following general inequality:

$$g(p_i) \leq 0 \quad (16)$$

where  $g(p_i)$  is an inequality that can be used instead of a boundary constraint. In other words,  $p_i(t)$  runs all the way through its range of maximum  $p_i^{\max}$  and minimum values  $p_i^{\min}$ , so we can defined the range of  $p_i(t)$  to be  $\Omega_i = \{x_i | g(x_i) \leq 0\}$ .

According to the Lagrange multiplier method, we can obtain the Lagrange function of objective (11)–(15) as:

$$L(p, \lambda) = \sum_{i=1}^n L_i(p_i, \lambda) = \sum_{i=1}^n f_i(p_i) + \sum_{i=1}^n \lambda_i h_i(x_i) \tag{17}$$

where  $h_i(x_i) = p_i - l_i$ ,  $\lambda_i$  is the Lagrange multiplier which has the physical meaning of the price of electricity generation. We define that  $\lambda_i^*$  is the optimal solution of  $\lambda_i$ ,  $p^* = [p_1^*, \dots, p_{n+m+w}^*]$  is the optimal solution vector of  $p_i(t)$ . To ensure that (17) has a feasible solution, we formulate Assumption 1 such that there exists a Slater vector for (17).

Assumption 1: In the function (17), there exists a vector  $p^* \in p$  such that  $g_\pi(p^*) < 0$  for all  $\pi = 1, 2, \dots, \gamma$ .

We introduce the box projection to solve the inequality constraint (16). The principle of box projection is to find the minimum distance from a point to any point in the feasible domain, which obtains a feasible point in the feasible domain. The projection operation of  $p$  on  $\Omega = \{p \in \mathbb{R} | p^{\min} \leq p \leq p^{\max}\}$  comes from  $P_\Omega(p) = \operatorname{argmin}_{x \in \Omega} \|p - \tilde{x}\|$ . In the latter, we introduce the sign function  $\operatorname{sign}(a)$ , which serves to replace the value of variables using a step signal, and thus enables positive and negative determinations. The sign function is defined as:

$$\operatorname{sign}(a) = \begin{cases} 1 & \text{if } a > 0 \\ 0 & \text{if } a = 0 \\ -1 & \text{if } a < 0 \end{cases}$$

### 3.2 Surplus-Based Algorithm

For problems (11)–(15), existing distributed optimization algorithms are deficient in handling directed graphs and general convex optimization problems. In this section, we propose a surplus-based fully distributed event-triggered optimization algorithm, drawing on continuous-time gradient descent [9] and ADMM algorithms [10]. The specific form of the algorithm is as follows:

$$\begin{aligned} \dot{p}_i(t) = & -\alpha(t)(\nabla f_i(p_i(t)) + \lambda_i(t)) \\ & + |-\alpha(t)(\nabla f_i(p_i(t)) + \lambda_i(t))| \cdot \operatorname{sign}(P_{\Omega_i}(p_i(t)) - p_i(t)) \\ & + k_1 \operatorname{sig}(P_{\Omega_i}(p_i(t)) - p_i(t))^u + k_2 \operatorname{sig}(P_{\Omega_i}(p_i(t)) - p_i(t))^v \end{aligned} \tag{18}$$

$$\begin{aligned} \dot{\lambda}_i(t) = & \Lambda_i(t) + \varepsilon y_i(t) + \alpha(t)(p_i(t) - l_i) \\ & + |\tilde{\Lambda}_i(t) + \varepsilon y_i(t) + \alpha(t)(p_i(t) - l_i)| \cdot \operatorname{sign}(P_{\Theta_i}(\lambda_i(t)) - \lambda_i(t)) \\ & + k_1 \operatorname{sig}(P_{\Theta_i}(\lambda_i(t)) - \lambda_i(t))^u + k_2 \operatorname{sig}(P_{\Theta_i}(\lambda_i(t)) - \lambda_i(t))^v \end{aligned} \tag{19}$$

$$\dot{y}_i(t) = -d_i^{\text{out}} y_i(t^m) + \sum_{j \in N_i} a_{ij} y_j(t_j^m) - \varepsilon y_i(t) - \Lambda_i(t) \tag{20}$$

$$\Lambda_i(t) = \sum_{j \in N_i} a_{ij} (\lambda_j(t_j^m) - \lambda_i(t_i^m)) \tag{21}$$

where  $\alpha(t)$  is a non-increasing gain parameter satisfying  $\int_0^\infty \alpha(t) dt = \infty$ , and  $\int_0^\infty \alpha^2(t) dt < \infty$  i.e., we can assume  $\alpha(t) = 50/(10 + 3t)$ . Where  $\text{sig}(a)^b = [\text{sign}(a_1) |a_1|^b, \dots, \text{sign}(a_n) |a_n|^b]^T$ , and  $\text{sign}(a)$  is the sign function.  $p_i(t)$  is the output of distributed generation which is computed locally.  $\lambda_i$  and  $y_i$  follow the neighbor information interaction as shared variables.  $k_1 > 0, k_2 > 0, 0 < \mu < 1$ , and  $\nu > 1$  are constants.  $t_i^m$  represents  $m$ th triggering time.  $P_{\Omega_i}(p_i)$  and  $P_{\Theta_i}(\lambda_i)$  represent the box-projection operation of  $p_i$  and  $\lambda_i$  in the local constraint interval  $\Omega_i$  and set  $\Theta_i$ , respectively.

In the proposed algorithm, Eq. (18) computes the target variable locally and is not involved in information transfer. Eqs. (19), (20) participate in information transfer and compute the sharing variables  $\lambda_i$  and  $y_i$  through neighbor node information. During the algorithm design process, Eq. (18) utilizes  $(\nabla f(p_i(t)) + \lambda_i(t))$  to calculate the gradient descent of the dual problem of (17). To handle the inequality constraint, we employ the incentive projection, as demonstrated in the remaining terms of the equation. To ensure convergence, the second term of (18) is included, while  $k_1 \text{sig}(P_{\Omega_i}(p_i(t)) - p_i(t))^\mu$  and  $k_2 \text{sig}(P_{\Omega_i}(x_i(t)) - x_i(t))^\nu$  guarantee that  $p_i$  converges to the feasible region  $\Omega_i$  within a fixed time. Additionally, Eq. (18) is utilized for local updates of the state variable  $p_i$ , and information exchange among neighbors is facilitated through  $y_i$  and  $\lambda_i$ . Sensitive information is protected while recording system deviations. Furthermore, the  $\lambda_i$  variable acts as a Lagrangian dual variable, assisting with equation constraint (13). Eq. (19) is employed to update  $\lambda_i$ , which consists of three components: the consistency protocol, eigenvalue perturbation, and incentive projection. The consistency protocol  $\Delta_i$  drives all  $\lambda_i$  values towards a common value. This allows the auxiliary variable  $y_i$  to track changes in the dual variable  $\lambda_i$  and compensate for any unbalanced impact caused by the directed graph.

The pseudo-code of this algorithm is shown in Algorithm 1, where the current generation power of the devices such as photovoltaic and energy storage and the parameters used in the algorithm are first entered, where the algorithm parameters are arbitrary values. Based on the information transfer between neighboring nodes, the values of variables  $p, \lambda$  and  $y$  are calculated continuously using algorithm (18)–(21). When the algorithm converges, the value of variable  $p$  is the optimal generation power.

---

**Algorithm 1:** Surplus-Based Distributed Optimization Algorithm

---

Input: Local loads  $d_i$ , Lagrange matrix  $L$  of communication network. Any admissible values of  $p_i(0), \lambda_i(0), y_i(0)$ .

While unconvergence do

Exchange data  $\lambda_i, y_i$  with neighbor nodes.

Execute surplus-based distributed optimization algorithm (18)–(21).

End

Output: The optimal output of each power devices.

---

Information interactions between nodes incur communication costs, i.e., the resources and costs consumed when communicating, such as bandwidth consumption, communication frequency, etc. So, the event triggering mechanism is introduced to reduce communication costs. Event triggering mechanism from the system's performance and stability, before the start of the system to set a trigger threshold in advance, so that when the state of the system does not change much when it is not sampling and transmission, only when the system state changes over the set threshold will carry out the corresponding action that is, the data sampling and transmission, which greatly saves the communication resources to reduce the burden on the network. The local processor will pay attention to the variables  $a, b$  and  $c$  in real time. A trigger function is used to decide whether to interact with the information or not, and whether to use the local history information or the neighbor node information



for the next computation. The trigger function is defined as follows:

$$\mathcal{C}_1(\lambda_i(t_i), y_i(t_i)) = a_3 \left( \varpi_1 \|\lambda_i(t_i^m) - \lambda_i(t_i)\|^2 + \varpi_2 \|y_i(t_i^m) - y_i(t_i)\|^2 - \frac{1}{2a_1} \sum_{i \in N_i} a_{ij} \|\lambda_i(t_i^m) - \lambda_i(t_j^m)\|^2 \right) \tag{22}$$

$$\mathcal{C}_2(\lambda_i(t_i)) = |\lambda_i^m(t) - \lambda_i(t)| - \alpha(t) e^{-\sigma t} \tag{23}$$

$$\mathcal{C}_3(y_i(t_i)) = |y_i^m(t) - y_i(t)| - \alpha(t) e^{-\sigma t} \tag{24}$$

$$\mathcal{C} = \min \{ \mathcal{C}_1(\lambda_i, y_i), \mathcal{C}_2(\lambda_i), \mathcal{C}_3(y_i) \} \tag{25}$$

where  $\mathcal{C}_1(\lambda_i(t_i), y_i(t_i))$ ,  $\mathcal{C}_2(\lambda_i(t_i))$  and  $\mathcal{C}_3(y_i(t_i))$  are parallel trigger functions representing neighbor information mismatch,  $\lambda_i$  mismatch and  $y_i$  mismatch, respectively.  $\varpi_1 = [2(a_1 - 1)/a_1 + a_2] |N_i|$ ;  $\varpi_2 = a_2 |N_i|$ ;  $a_1, a_2, a_3, \pi$ , and  $\sigma$  are positive constants. The proposed event triggering method is a parallel triggering mechanism. Eq. (25) is the main trigger basis. Since (25) is equal to the smallest value in (22)–(24), the local dynamic update is considered to reach the threshold when any of (22)–(24) is a non-positive number. The main purpose of the trigger function (22)–(24) is to ensure that the algorithm (18)–(21) achieves large-scale asymptotic convergence and triggers information interactions when the algorithm tends to diverge. The form of its expression and the range of threshold selection can be justified from the convergence and optimal solution proofs in the later sections. Also, the threshold  $\mathcal{C}$  is time-varying because the trigger function contains  $\lambda_i(t_i), y_i(t_i)$  variables. The communication system will exchange the neighbor information in the next moment and the algorithm (18)–(21) will use the new data to complete the dynamic update. Based on (22)–(25), the next triggering time is determined as:

$$t_i^{m+1} = \max \{ t \geq t_i^m | \mathcal{C}(\lambda_i(t_i), y_i(t_i)) \leq 0 \} \tag{26}$$

The proposed distributed algorithm increases the reliability, robustness, flexibility and privacy preservation in the economic dispatch process of smart grid. First, the algorithm is based on the information interaction between neighboring nodes, which reduces the impact of a single point of failure on the system, as long as the communication network is fully connected. Second, this algorithm operates in a fully distributed approach where any single point or channel can join the system directly, perfectly matching the hot-plugging property of smart grids, thus enhancing the flexibility of the system. Third, the auxiliary variables are transmitted among neighboring nodes as shared variables and the target variables are computed locally. This dynamic update method protects the privacy of the target variables and reduces the risk of information leakage. To minimize the communication frequency within the network, we have incorporated an event-triggering mechanism into the surplus optimization algorithm. Reducing the communication cost also reduces the possibility of packet loss or information leakage.

### 3.3 Optimality and Convergence Analysis

In this subsection, we demonstrate the convergence and optimality of the algorithm using Lyapunov functions, linearized scaling, and finite-time projection. To eliminate the effect of inequality constraints on the optimization algorithm we first introduce Lemma 1, which demonstrates the convergence of the algorithm within a fixed time. This convergence is achieved through the utilization of symbolic functions and projection operations, as outlined below:

**Lemma 1:** Suppose that the  $f(p_i)$  function is both strongly convex and Lipschitz continuous. In a fixed time, the variables  $p_i$  and  $\lambda_i$  converge to  $\Omega_i$  and  $\Theta_i$ , respectively.

*Proof:* Defined the Lyapunov function is  $V_1 = (p_i - P_\Omega(p_i))^2$ . We can get Lie derivative of  $V_1$  as follows:

$$\begin{aligned} \dot{V}_1 &\leq -k_1 |P_\Omega(p_i) - p_i|^{u+1} - k_2 |P_\Omega(p_i) - p_i|^{v+1} \\ &\leq -k_1 V_1^{\frac{u+1}{2}} - k_2 V_1^{\frac{v+1}{2}} \leq 0 \end{aligned} \quad (27)$$

Based on Lemma 1 in [17], the equation above indicates that  $V_1$  can converge to 0 when  $t = \{t \geq T_1 | T_1 \leq 1/k_1(1-u) + 1/k_2(1-v)\}$ . Consequently, we can deduce that  $p_i(t) = P_\Omega(p_i(t))$  holds true for  $t \geq T_1, \forall i$ . Similarly, by selecting the Lyapunov function as  $V_2 = (\lambda_i - P_{\Theta_i}(\lambda_i))^2$ , we can get  $\lambda_i = P_{\Theta_i}(\lambda_i)$ . This completes the proof.

By Lemma 1, we can get  $p_i(t) = P_\Omega(p_i(t))$  and  $\lambda_i = P_{\Theta_i}(\lambda_i)$  when the fixed time projection is completed. After the moment  $T_1$ , algorithm (18)–(21) can be transformed as follows:

$$\begin{aligned} \dot{p}_i(t) &= -\alpha(t) (\nabla f_i(p_i(t)) + \lambda_i(t)) \\ \dot{\lambda}_i(t) &= \Lambda_i(t) + \varepsilon y_i(t) + \alpha(t) (p_i(t) - l_i) \\ \dot{y}_i(t) &= -d_i^{out} y_i(t^m) + \sum_{j \in N_i} a_{ij} y_j(t^m) - \varepsilon y_i(t) - \Lambda_i(t) \end{aligned} \quad (28)$$

In other words, both  $p_i$  and  $\lambda_i$  are within the boundaries  $\Omega_i$  and  $\Theta_i$  when  $t \geq T_1$ . The inequality constraint (14) has been solved. Meanwhile, since the renewable energy uncertainty is transformed into the operational boundary constraint  $[\bar{p}_{i,t}^{PV}, \underline{p}_{i,t}^{PV}]$ , the boundary problem is solved implying that the renewable energy uncertainty is eliminated when  $t \geq T_1$ . This specific fixed-time projection eliminates inequality constraints while harmonizing the incompatibility of uncertainty, compensation cost, power and cost in the same objective function. By algorithm (28), we can conclude that as  $t \rightarrow \infty, L\lambda \rightarrow 0$  and  $y_i(t) \rightarrow 0$  for all  $i$ . Let us denote the equilibrium point of (11)–(15) as  $(p_i^*, \lambda_i^*, y_i^*)$ . To further facilitate the analysis, we introduce three auxiliary variables as follows:

$$\begin{aligned} \Pi(t) &= (p(t) - p^*), \eta(t) = (\lambda(t) - \lambda^*) \\ \Xi(t) &= (y(t) - y^*), e(t) = \eta(t^m) - \eta(t) \\ z(t) &= \Xi(t^m) - \Xi(t) \end{aligned} \quad (29)$$

where  $p^*, \lambda^*$ , and  $y^*$  are the compact forms of  $p_i^*, \lambda_i^*$ , and  $y_i^*$ , respectively. Next, the following Lemma 2 illustrates the convergence and optimality of the proposed algorithm (11)–(15):

**Lemma 2:** Assuming that the directed graph  $G$  is connected, algorithm (28) will asymptotically converge to  $(p_i^*, \lambda_i^*, y_i^*)$ . Furthermore,  $p^*$  represents the optimal solution of problem (11)–(15).

*Proof:* we define the Lyapunov function as follows:

$$V_3(t) = \frac{1}{2} (\|\Pi(t)\|^2 + \|\eta(t)\|^2 + \|\Xi(t)\|^2) \quad (30)$$

Based on (28)–(29), the Li derivatives of Lyapunov function (30) is as follows:

$$\begin{aligned}
 \dot{V}_3(t) &= \Pi^T(t) \dot{\Pi}(t) + \eta^T(t) \dot{\eta}(t) + \Xi^T(t) \dot{\Xi}(t) \\
 &= \eta^T(t) (-L\lambda(t^m) - \alpha(t) \Pi^T(t) (-\nabla f(x(t)) + \lambda(t)) \\
 &\quad + \Xi^T(t) (L'\lambda^m - L'y(t^m) - \varepsilon y(t)) + \varepsilon y(t) + \alpha(t) (p(t) - l)) \\
 &= -\alpha(t) \Pi^T(t) (\nabla f(p(t)) + \nabla f(p^*)) \\
 &\quad - \eta^T(t) L(\lambda(t^m) - \lambda^*) - \alpha(t) \Pi^T(t) \eta(t) \\
 &\quad + \alpha(t) \eta^T(t) \Pi(t) + \varepsilon \eta^T(t) \Xi(t) \\
 &\quad - \Xi^T(t) L'(y(t^m) - y^*) - \varepsilon \Xi^2(t) + \Xi^T(t) L(\lambda(t^m) - \lambda^*)
 \end{aligned} \tag{31}$$

where  $\zeta = \text{diag}\{\zeta_i\}$  is the general convex coefficient of the convex function  $f(x(t))$ , we can obtain  $\alpha(t) \Pi^T(t) R^T(-\nabla f(x(t)) + \nabla f(x^*)) \leq -\alpha(t) \Gamma^T(t) \zeta \Gamma(t)$  from the properties of convex functions. Since the Laplace matrix  $L$  and  $L'$  are positive definite, there exists a minimum nonzero eigenvalue  $\kappa_2$  and  $\kappa'_2$ . We can further get  $\lambda^T(t) L\lambda(t) \geq \kappa_2 \|\lambda(t)\|^2$  and  $\eta^T(t) L'\eta(t) \geq \kappa'_2 \|\eta(t)\|^2$ . Based on Young's inequality, one obtains  $\Pi^T(t) \eta(t) = 2\|\Pi(t)\|^2 + \|\eta(t)\|^2/2$ . According to the (29) and definition of  $N_i$ , it not hard to prove  $e^T(t) L e(t) \leq 2 \sum_{i=1}^n |N_i| \cdot \|\lambda_i(t_i^m) - \lambda_i(t_i)\|^2$  and  $z^T(t) L' z(t) \leq 2 \sum_{i=1}^n |N_i| \cdot \|y_i(t_i^m) - y_i(t_i)\|^2$ . Based on convex and graph theory, each term in (31) can be replaced by (29). Since  $\varepsilon$  and  $\alpha(t)$  is non-negative, it can be derived to following inequality by deflation:

$$\begin{aligned}
 \dot{V}_3(t) &\leq -\alpha(t) \zeta \|\Pi(t)\|^2 \\
 &\quad - \left[ \left( \frac{a_1 - 2}{2a_1} \right) \kappa_2 - \frac{\varepsilon}{2} \right] \|\eta(t)\|^2 - \left[ \frac{\varepsilon}{2} - \frac{\kappa_2}{2a_2} \right] \|\Xi(t)\|^2 \\
 &\quad + a_3(\varpi_1 \|e(t)\|^2 + \varpi_2 \|z(t)\|^2) \\
 &\quad - \frac{1}{2a_1} \sum_{i=1}^n \sum_{j \in N} a_{ij} \|\lambda_i(t_i^m) - \lambda_j(t_j^m)\|^2
 \end{aligned} \tag{32}$$

where  $a_1 \geq (1 - \varepsilon)/(2\kappa_2)$  and  $a_2 \geq \kappa_2/\varepsilon$ . According to the triggering strategy (22)–(25), we have:

$$a_3(\varpi_1 \|e(t)\|^2 + \varpi_2 \|z(t)\|^2) - \frac{1}{2a_1} \sum_{i=1}^n \sum_{j \in N} a_{ij} \|\lambda_i(t_i^m) - \lambda_j(t_j^m)\|^2 \leq 0 \tag{33}$$

So, by the previous definitions of  $a_1, a_2, \varpi_1, \varpi_2$ , we can have  $\dot{V}_3(t) \leq 0$ . Thus, when  $t \rightarrow \infty$ , algorithm (18)–(21) achieves  $p = p^*$ . Further, through the above analysis we can easily get:

$$\begin{aligned}
 \sum_{i=1}^n p_i^* &= \sum_{i=1}^n l_i \\
 \lambda_i^* &= \lambda_j^* \\
 \sum_{i=1}^n f_i(p_i^*) &= L(p^*, \lambda^*)
 \end{aligned} \tag{34}$$

In summary, Eq. (34) satisfies the Karush-Kuhn-Tucker (KKT) conditions for the Lagrangian function (17) and algorithm (18)–(21) converges asymptotically to  $p = p^*$ . Therefore, we consider  $p^*$  to be the globally optimal solution. This completes the proof.

### 4 Simulation and Results

We adopt a smart grid distribution topology consisting of 40 buses and 10 energy devices, as illustrated in Fig. 1. The physical structure of the network includes 6 DFGs, 2 DRGs, and 2 DPSDs in Table 2. The energy transmission network is represented by solid lines, while the directed information transmission network is represented by dotted lines. To ensure consistency in units, we define 1 p.u. as 1 MW for power and 1 p.u. as 1 \$/MWh for price [22]. The scalability of the proposed distributed event-triggered surplus algorithm is demonstrated on this large urban network with 40 buses. Additionally, all simulation are running on a server computer with Win10, i7-10700K CPU @ 3.80 GHz and 64 GB RAM.

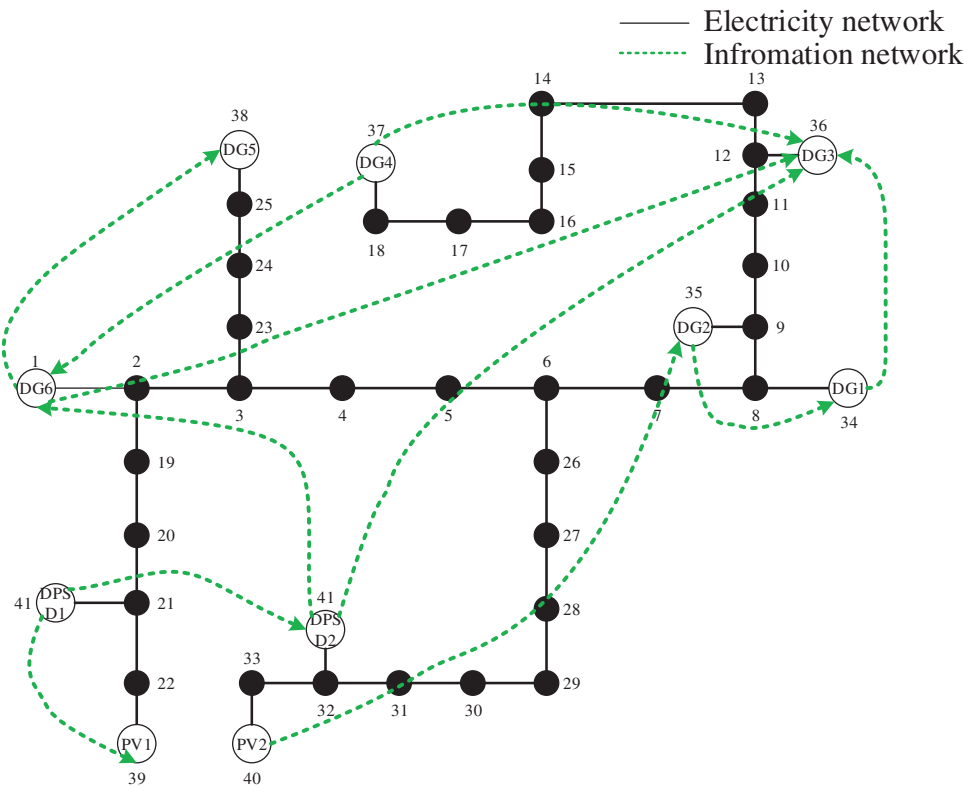


**Figure 1:** The network of the 119-bus test system

**Table 2:** Parameters of the test system

	a	b	c
DFG1	0.021	7.88	80
DFG2	0.01	7.85	85
DFG3	0.022	7.8	100
DFG4	0.031	7.82	130
DFG5	0.025	7.79	83
DFG6	0.019	7.87	110

(Continued)

<b>Table 2 (continued)</b>			
	a	b	c
DRG1	0.29	4.5	0.4
DRG2	0.17	3.9	0.4
DPSD1	0.031	16	
DPSD2	0.029	18	

**4.1 Result and Analysis of Distributed Event-Triggered Surplus Algorithm**

This subsection investigates the convergence of the proposed algorithm. The power load for the information network consisting of 10 nodes is initially set to 22.4 p.u. During the computation, data is exchanged among neighboring energy devices in the smart grid. The proposed algorithm calculates the local target variable in a distributed manner, using arbitrarily selected initial values.

Fig. 2 verifies that the proposed algorithm can achieve the supply and demand balance of the system. Where the curve  $mismatch = \sum_{i=1}^{n+m+w} p_i - \sum_{i=1}^{n+m+w} l_i$ . When  $t = 10$  the curve reaches 0, indicating that the current state has satisfied the equation constraints (13). However, at this time, each power generating device is not the optimal output state, i.e., it does not satisfy the social welfare maximization. So the distributed computing needs to continue to run. Fig. 3 shows that the surplus of this algorithm gradually reaches 0 at  $t = 15$ . indicating that at this point the algorithm has eliminated the local bias. All subsequent computations satisfy the inequality constraint (14), (15). In addition, Fig. 4 illustrates the trend of all target variables  $p_i$ . After the distributed computation, all devices reach the optimal power generation. At this time, the smart grid system realizes the global supply and demand balance (13), and the local devices satisfy the local inequality constraints (14), (15). Meanwhile the system maximizes the welfare.

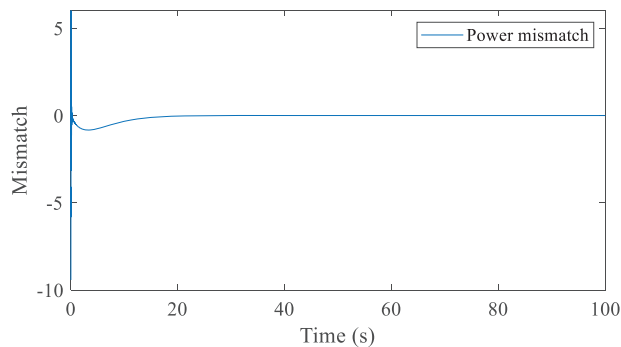


**Figure 2:** Power mismatch by using the proposed method

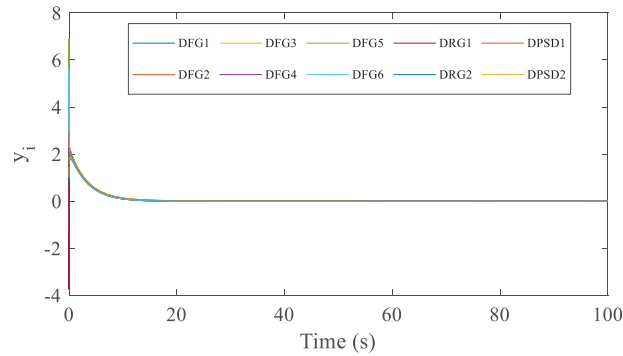


**Figure 3:** Energy surplus by using the proposed method

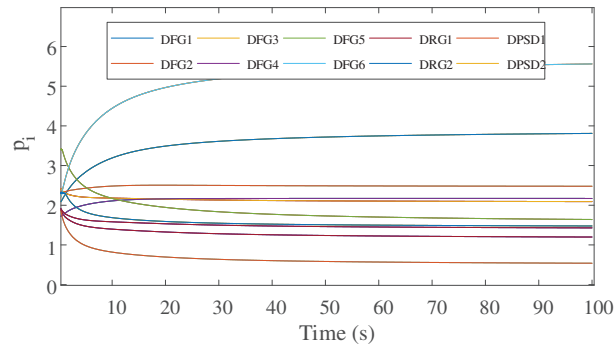


**Figure 4:** Energy output by proposed algorithm

#### 4.2 Event-Triggered and Hot-Plug Performance Analysis

In this section, the event-triggered and hot-plugging characteristic of the distributed event-triggered surplus algorithm is analyzed by using the topology and data from the previous section as Fig. 2 and Table 1. Fig. 5 displays the event-triggered sequence of each distributed generation devices, with each triggering time denoted by “†”. For better observation, the period between 25 and 40 in Fig. 5 is enlarged on the right side. It can be found that the information transfer between neighboring nodes is not continuous but discrete and asynchronous. The proposed algorithm communicates only at the triggering moment to achieve the update of node interaction information. This greatly reduces the frequency and cost of communication. In addition, since the threshold of the trigger function (22)–(24) is continuously decreasing with the value of  $p_i$ ,  $\lambda_i$  and  $y_i$ , it can be guaranteed that the event triggering mechanism is continuously running.

The hot-plugging performance of this algorithm is demonstrated in Fig. 6. The total load of the power system is initially set to 22.4. when the system is gradually stabilized, the total load is adjusted to 17 at the 50 s. It can be found that the curve fluctuates at the 50 s, and gradually returns to smoothness at the 90 s. At this time, all the DG, PV and storage outputs reach the optimum and ensure the supply and demand of the system. At this time, the outputs of all DG, PV and storage reach their optimal values and ensure the balance between supply and demand of the system. And then, at 100 s, DG1 and PV1 are cut off and the curve fluctuates at the same time. Since this algorithm is a fully distributed algorithm, a single point of failure does not affect the distributed optimization calculation

of the remaining devices. At 130 s, the curves of the remaining 8 devices are restored to be stable. The output of all devices reaches the optimal value and the system supply-demand balance is realized.

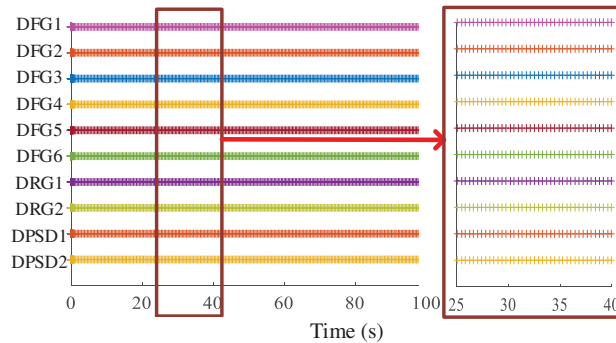


**Figure 5:** Event triggering sequence

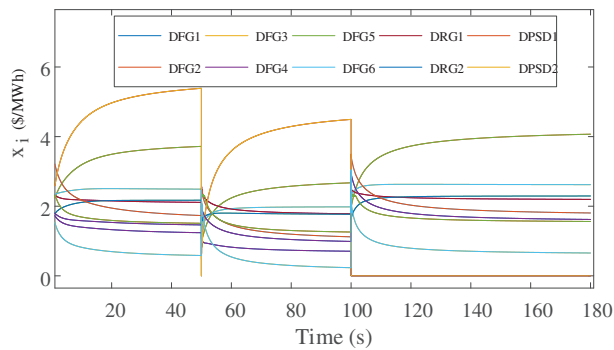


**Figure 6:** Curves for hot-plug

Compared with the continuous time algorithm in literature [9], this paper incorporates the event-triggered mechanism on the basis of its algorithm, which makes the information transmission of neighboring nodes discrete and avoids the exchange of continuous state information in literature [9]. Literature [9] is mainly aimed at the economic scheduling problem with the smart grid, compared with literature [9], this paper is specifically for the economic scheduling problem of photovoltaic power generation and energy storage devices, but this paper’s simulation experimental result of hot-plug is consistent with the plug-and-play characteristic of economic scheduling to meet the literature [9], which illustrates the effectiveness of this paper’s distributed optimization algorithm, which is able to solve the problem of the economic scheduling of photovoltaic power generation and energy storage devices very well.

### 5 Conclusion

This paper introduces a novel renewable energy cost model and a distributed optimization algorithm tailored for the economic dispatch challenge within smart grids. In order to integrate renewable energy into economic dispatch, this paper models the operating cost of renewable energy by introducing penalty factors and confidence intervals. Cost compensation is utilized to compensate for the renewable energy forecasting output error due to uncertainty. The cost compensation increases with the increase of prediction error. Meanwhile, a distributed event-triggered surplus optimization

algorithm is proposed in this paper. The algorithm increases the stability, flexibility, robustness and privacy protection of the system with a unique dynamic update rule. In addition, this paper provides complete convergence and optimality proofs.

**Acknowledgement:** None.

**Funding Statement:** The Science and Technology Project of the State Grid Corporation of China (Research and Demonstration of Loss Reduction Technology Based on Reactive Power Potential Exploration and Excitation of Distributed Photovoltaic-Energy Storage Converters: 5400-202333241A-1-1-ZN).

**Author Contributions:** The paper was conceptualized by KC.L. and methodologically developed by C.L. and NY.W. The first draft was written by XY.D. and C.L., while programming and manuscript writing were done by H.Y. All authors reviewed the results and approved the final version of the manuscript.

**Availability of Data and Materials:** The data that support the findings of this study are available from the corresponding author, Hui Yu, upon reasonable request.

**Conflicts of Interest:** The authors declare that they have no conflicts of interest to report regarding the present study.

## References

1. W. Zheng and D. J. Hill, "Distributed real-time dispatch of integrated electricity and heat systems with guaranteed feasibility," *IEEE Trans. Ind. Inf.*, vol. 18, no. 2, pp. 1175–1185, 2022. doi: [10.1109/TII.2021.3083653](https://doi.org/10.1109/TII.2021.3083653).
2. A. Q. Huang, M. L. Crow, G. T. Heydt, J. P. Zheng, and S. J. Dale, "The future renewable electric energy delivery and management system: The energy internet," *Proc. IEEE*, vol. 99, no. 1, pp. 133–148, 2011. doi: [10.1109/JPROC.2010.2081330](https://doi.org/10.1109/JPROC.2010.2081330).
3. Q. Chen, Z. Kuang, X. Liu, and T. Zhang, "Energy storage to solve the diurnal, weekly, and seasonal mismatch and achieve zero-carbon electricity consumption in buildings," *Appl. Energy*, vol. 312, no. 18, pp. 118744, 2022. doi: [10.1016/j.apenergy.2022.118744](https://doi.org/10.1016/j.apenergy.2022.118744).
4. H. Wang, C. Gu, X. Zhang, and F. Li, "Optimal CHP planning in integrated energy systems considering network charges," *IEEE Syst. J.*, vol. 14, no. 2, pp. 2684–2693, 2022. doi: [10.1109/JSYST.2019.2921218](https://doi.org/10.1109/JSYST.2019.2921218).
5. Z. Chen, Y. Zhang, T. Ji, Z. Cai, L. Li and Z. Xu, "Coordinated optimal dispatch and market equilibrium of integrated electric power and natural gas networks with P2G embedded," *J. Mod. Power Syst. Clean Energy*, vol. 6, no. 3, pp. 495–508, 2018. doi: [10.1007/s40565-017-0359-z](https://doi.org/10.1007/s40565-017-0359-z).
6. N. G. Kiryanova, P. V. Matrenin, S. V. Mitrofanov, S. E. Kokin, and M. K. Safaraliev, "Hydrogen energy storage systems to improve wind power plant efficiency considering electricity tariff dynamics," *Int. J. Hydrogen Energy*, vol. 47, no. 18, pp. 10156–10165, 2022. doi: [10.1016/j.ijhydene.2022.01.152](https://doi.org/10.1016/j.ijhydene.2022.01.152).
7. C. Zhao, J. He, and P. Cheng, "Analysis of consensus-based distributed economic dispatch under stealthy attacks," *IEEE Trans. Ind. Electron.*, vol. 64, no. 6, pp. 5107–5117, 2017. doi: [10.1109/tie.2016.2638400](https://doi.org/10.1109/tie.2016.2638400).
8. Z. Zhang and M. Y. Chow, "Convergence analysis of the incremental cost consensus algorithm under different communication network topologies in a smart grid," *IEEE Trans. Power Syst.*, vol. 27, no. 4, pp. 1761–1768, 2012. doi: [10.1109/tpwrs.2012.2188912](https://doi.org/10.1109/tpwrs.2012.2188912).
9. S. Yang, S. Tan, and J. Xu, "Consensus based approach for economic dispatch problem in a smart grid," *IEEE Trans. Power Syst.*, vol. 28, no. 4, pp. 4416–4426, 2013. doi: [10.1109/tpwrs.2013.2271640](https://doi.org/10.1109/tpwrs.2013.2271640).



10. G. Binetti, A. Davoudi, D. Naso, B. Turchiano, and F. L. Lewis, "A distributed auction-based algorithm for the nonconvex economic dispatch problem," *IEEE Trans. Ind. Inf.*, vol. 10, no. 2, pp. 1124–1132, 2014. doi: [10.1109/tii.2013.2287807](https://doi.org/10.1109/tii.2013.2287807).
11. N. Rahbari-Asr, U. Ojha, Z. Zhang, and M. Y. Chow, "Incremental welfare consensus algorithm for cooperative distributed generation/demand response in smart grid," *IEEE Trans. Smart Grid*, vol. 5, no. 6, pp. 2836–2848, 2014. doi: [10.1109/TSG.2014.2346511](https://doi.org/10.1109/TSG.2014.2346511).
12. X. He, Y. Zhao, and T. Huang, "Optimizing the dynamic economic dispatch problem by the distributed consensus-based ADMM approach," *IEEE Trans. Ind. Inf.*, vol. 16, no. 5, pp. 3210–3221, 2020. doi: [10.1109/TII.2019.2908450](https://doi.org/10.1109/TII.2019.2908450).
13. A. Attarha, P. Scott, and S. Thibaux, "Affinely adjustable robust ADMM for residential DER coordination in distribution networks," *IEEE Trans. Smart Grid*, vol. 11, no. 2, pp. 1620–1629, 2020. doi: [10.1109/TSG.2019.2941235](https://doi.org/10.1109/TSG.2019.2941235).
14. Y. Li, D. W. Gao, W. Gao, H. Zhang, and J. Zhou, "A distributed doubnewton descent algorithm for cooperative energy management of multiple energy bodies in energy internet," *IEEE Trans. Ind. Inf.*, vol. 17, no. 9, pp. 5993–6003, 2021. doi: [10.1109/TII.2020.3029974](https://doi.org/10.1109/TII.2020.3029974).
15. Y. Li, D. W. Gao, W. Gao, H. Zhang, and J. Zhou, "Double-mode energy management for multi-energy system via distributed dynamic event-triggered newton-raphson algorithm," *IEEE Trans. Smart Grid*, vol. 11, no. 6, pp. 5339–5356, 2020. doi: [10.1109/TSG.2020.3005179](https://doi.org/10.1109/TSG.2020.3005179).
16. X. Le, S. Chen, F. Li, Z. Yan, and J. Xi, "Distributed neurodynamic optimization for energy internet management," *IEEE Trans. Syst. Man Cybern.: Syst.*, vol. 49, pp. 1624–1633, 2019. doi: [10.1109/tsmc.2019.2898551](https://doi.org/10.1109/tsmc.2019.2898551).
17. Q. Liu, S. Yang, and J. Wang, "A collective neurodynamic approach to distributed constrained optimization," *IEEE Trans. Neu. Net. Learn. Syst.*, vol. 28, no. 8, pp. 1747–1758, 2017. doi: [10.1109/TNNLS.2016.2549566](https://doi.org/10.1109/TNNLS.2016.2549566).
18. G. Chen and Z. Li, "Distributed optimal resource allocation over strongly connected digraphs: A surplus-based approach," *Automatica*, vol. 125, pp. 109459, 2021. doi: [10.1016/j.automatica.2020.109459](https://doi.org/10.1016/j.automatica.2020.109459).
19. S. Liang, L. Wang, and G. Yin, "Distributed quasi-monotone subgradient algorithm for nonsmooth convex optimization over directed graphs," *Automatica*, vol. 101, no. 11, pp. 175–181, 2019. doi: [10.1016/j.automatica.2018.11.056](https://doi.org/10.1016/j.automatica.2018.11.056).
20. R. Ren, Y. Li, Q. Sun, S. Zhang, D. W. Gao and S. Maharjan, "Switched surplus-based distributed security dispatch for smart grid with persistent packet loss," *IEEE Internet Things J.*, vol. 11, no. 4, pp. 6185–6198, 2024. doi: [10.1109/JIOT.2023.3311758](https://doi.org/10.1109/JIOT.2023.3311758).
21. Y. Li *et al.*, "Distributed hybrid-triggering-based secure dispatch approach for smart grid against DoS attacks," *IEEE Trans. Syst. Man Cyber.: Syst.*, vol. 53, no. 6, pp. 3574–3587, 2023. doi: [10.1109/TSMC.2022.3228780](https://doi.org/10.1109/TSMC.2022.3228780).
22. M. Wang, Y. Wu, M. Yang, M. Wang, and L. Jing, "Dynamic economic dispatch considering transmission distribution coordination and automatic regulation effect," *IEEE Trans. Ind. Appl.*, vol. 58, no. 3, pp. 3164–3174, 2022. doi: [10.1109/TIA.2022.3152455](https://doi.org/10.1109/TIA.2022.3152455).